



Research article

A multi-objective optimization model for green demand responsive airport shuttle scheduling with a stop location problem

Ming Wei¹, Congxin Yang¹, Bo Sun^{1,2,*} and Binbin Jing³

¹ CAAC Key Laboratory of Civil Aviation Wide Surveillance and Safety Operation Management & Control Technology, Civil Aviation University of China, Tianjin 300300, China

² School of Air Traffic Management, Civil Aviation University of China, Tianjin 300300, China

³ School of Transportation and Civil Engineering, Nantong University, Nantong 226019, China

* **Correspondence:** Email: bosun@cauc.edu.cn.

Abstract: We proposed a multi-objective optimization framework for green demand responsive airport shuttle scheduling, which simultaneously aims at assigning demand points to selected stops and routing airport shuttles to visit these stops in their overlapping time windows to transport all passengers from their homes or workplaces to the airport. Our objectives were to minimize total travel time for passengers, the punishment expense of violating the time-window as well as carbon emissions for all shuttles. Since such issues belongs to the NP-problem, a two-stage Multi-objective ant lion optimizer (MOALO)-based algorithm incorporating dynamic programming search method was developed to acquire the optimal scheduling schemes. Finally, a case study of airport shuttle service in Tianjin Airport, China, was used to demonstrate the validity of the model and algorithm.

Keywords: green demand responsive airport shuttle scheduling; stop location; two-stage heuristic approach

1. Introduction

There is a significant rise in the demand for air transportation due to global economic expansion, which has resulted in a sizable increase in traffic and passenger flows to the airport [1]. The growing demand for air transportation has led to an increasing interest in landside shuttle transit to airports. The current airport landside transportation services are primarily conventional shuttle bus and rail traffic

fitted in areas with large passenger flow. Nevertheless, this tends to generate large operational expenses and low levels of service in areas with low travel demand. With the support of information technology and smartphones, various scenarios emerge in the demand-responsive airport shuttle scheduling (DRASS), which operates in some low-density areas and offers flexible and personalized shuttle services [2]. Such potential advantages are likely to involve decreasing operating expense and carbon emissions as well as enhancing service level.

The DRASS system, where guests make trip requests via the smart phone and the company organizes shuttles to provide a shuttle service based on the real-time demand, is a significant part of the airport landside shuttle transportation system. Similar to the demand-responsive transit (DRT), green DRASS (GDRASS) is now a crucial concern due to raised environmental awareness. Under such a circumstance, the route planning of GDRASS decides the economic expense, service level as well as carbon emissions. Consequently, GDRASS differs from conventional systems, and studies that account for the influence of the environment on airport shuttle (AS) route design are necessary. Travel speed of shuttles is considered as a key factor for carbon emissions [3]. There are two primary types of studies on minimization of emissions in the DRASS model. The first group of models is on the hypothesis of constant AS speed, and the second group of models considers that the AS speed varies with time, depending on the road situation. Despite the fact that the first models are not precise, they are appropriate in the absence of historical data. Currently, remote vehicle tracking technology is utilized to gather extensive historical data under diverse traffic conditions, which is beneficial to precisely compute carbon emissions in the second model. Hence, it is meaningful to investigate the GDRASS model in a time-dependent environment to minimize pollution and damage to the environment.

Another significant observation was that traditional DRASS, which assumes that all demand points are served by shuttles, provide door-to-door services to passengers. In case of close distances between several demand points, the shuttle will cover a huge mileage, resulting in increased travel time. Under such circumstances, shuttles serve selected stops instead of demand points and passengers at demand points could interchange to selected stops to board the shuttle, which will dramatically enhance the level of service and decrease the sum of in-vehicle time for all passengers. Designing DRASS routes also requires assigning demand points to stops and selecting the optimal stops as pick-up sites [4,5]. Consequently, it is necessary to study demand-responsive airport shuttle route design with stop selection to weigh the relationship of operating expense, environmental expense and service levels.

The main contribution of this paper is to investigate a multi-objective optimization model for green DRASS with stop location under a time-dependent environment in order to minimize total travel time for passengers, carbon emissions and operational expense. Our major aims are concluded as below: (i) determination of the optimal design of GDRASS by simultaneously coordinating routing, departure time guidance and stop selection to balance service level and environmental conservation; (ii) creation of a MOALO-based heuristic approach to gain optimal scheduling schemes in a relatively short time. To demonstrate the validity of the GDRASS model and solution algorithm, an example in the actual world is presented at last.

The structure of the rest of this study is shown below: Section 2 provides an overview of relevant research regarding green DRASS; Section 3 describes the methodology of green DRASS with stop location under a time-dependent environment; Section 4 introduces a MOALO-based heuristic algorithm to settle the presented problem. Section 5 proves the applicability of the presented method with a practical example; Section 6 concludes the study and plans probable research directions in the future.

2. Related work

DRASS refers to assign all passengers in demand points to shuttles departing from various depots and plan routes to carry them from shuttle stops to the airport, which can be expressed as a variant of the vehicle routing problem (VRP) and the pick-up and delivery problem (PDP). Nevertheless, the obvious differences between VRP, PDP and DRASS lead to DRASS solving more problems with higher complexity than VRP and PDP. DRASS is more appropriate for areas with low population density, particularly those with poor transportation facilities, than fixed-route feeder transit services. Obviously, it, possessing a less operational cost and higher level of service, has appealed to many scholars from around the world come to study.

Generally speaking, DRASS need to pick up passengers within predefined time windows, which affects the quality of airport shuttle services. Many researchers have studied the airport shuttle scheduling with time windows and can be classified into hard time windows [5,6] and soft time windows [7–10]. The former requests airport shuttles must provide service to passengers within time window constraints, which means that vehicles should arrive at the pick-up locations between the earliest time of arrival and the latest time of departure. Sun et al. [5] presented a comprehensive optimal model for demand-responsive transportation in collaboration with shared bikes that can transport customs from demand points to the intersection of traffic with their service time windows. Xiao et al. [6] presented an optimal model for scheduling and route planning of green vehicles with time windows that takes carbon emissions into account. Nevertheless, arriving a few minutes late is acceptable if it does not affect the passenger's schedule. In the soft time window model, vehicles are permitted to arrive at stops out of the time window by charging a premium according to the time of early or delayed arrival. To solve the VRP with general soft time windows, Beheshti et al. [7] developed a new mixed-column generation-metaheuristic method. Wei et al. [8] presented an optimal model for demand-responsive airport bus with time-dependent speed. Xia et al. [9] developed a modified tabu searching method to settle open VRP with soft time windows. Xu et al. [10] investigated VRP with soft time windows based on fuzzy stochastic condition. Evidently, DRT and DRASS with soft time windows can enhance operational efficiency and decrease operational expense.

Currently, a new derivative of DRASS considering the environmental impact has drawn widespread attention. In this case, DRASS simultaneously considers the economic and environmental expense. In comparison to conventional problems, this will reduce carbon emissions, but add the economic expense. Most studies have only concentrated on carbon emissions minimizing vehicle routing [11,12]. For example, Zhang et al. [11] developed an environmentally friendly routing issue model with expenses of gasoline, carbon emissions and maintaining a vehicle as optimization objectives. Li et al. [12] took into account fuel and CO₂ emissions and built an emissions-based hybrid fixed fleet vehicle routing model. To decrease the expense of CO₂ emission, Wen et al. [13] investigated the multiple dispatch centers green vehicle routing issue. Integrated optimization models for vehicle routing and carbon emissions are seldom investigated [14]. Carbon emissions are determined by a variety of factors, but speed is the most significant one [15]. In previous DRASS problems, vehicle speed is usually considered to be constant, with little regard to reflecting real traffic conditions. The vehicle velocity is unlikely to remain fixed, and in the actual traffic network is continuously varying owing to various road environments at different times of the day [6]. In general, hypothetical distributions of fuzzy, grey and stochastic variables are usually acquired by utilizing previous datasets [16–18]. Nevertheless, piecewise functions can depict time-dependent speed more

accurately in the event of traffic data shortage [19]. As vehicle speed is substituted by the flow of traffic, these models are then developed as time-dependent DRASS [20,21]. Additionally, in time-dependent models, the speed of vehicles can be utilized as an added decision variable, which is beneficial in minimizing the total passengers' waiting time [22,23]. To address the limitation that a vehicle departing at a later time may exceed another vehicle that departed earlier, these models are built on the basis of the first-in-first-out (FIFO) or queuing theory [24,25].

The fundamental hypothesis of classical DRASS is that the pick-up locations are demand points [5]. In the case that some demand points are spatially adjacent, their travel time can be long in an actual traffic situation. As a matter of fact, a shuttle stop can satisfy the requirements of several neighboring demand points, and passengers at each demand point can select a neighboring stop to take the shuttle [26,27]. In general, the position of stops performs an essential role in the process of designing shuttle routes. Taking the features of the real traffic network into account, the selection of stops is on the basis of two principles: (i) reducing the interchange time of passengers between demand points and shuttle stops (ii) a high-efficiency shuttle route to service selected stops. Nevertheless, most studies have ignored comprehensive optimization of stop location and shuttle routing [2,4,8]. It is apparent that the allocation of demand points to selected stops is dictated by the location of the selected stops. As a result, coordinating stop location and the shuttle routing process has been generally recognized as an essential role in resolving DRASS.

From a literature review of DRASS, three key issues worth further research:

1) Most previous researches of DRASS assumed that all demand points were visited by ASs. The finding means ignoring the features of the actual traffic network. In real world, passengers at demand points are able to interchange to the closest stop to board the shuttle. In the case, integrated stop location and shuttle routing can effectively reduce passengers' total travel time and enhance the service level of ASs.

2) Few literatures have investigated how the time-dependent traffic environment and soft time windows affect AS scheduling and route planning, resulting in lacking of a comprehensive scheme that trades off carbon emissions and operating expense.

3) The conventional GRASS solution algorithm cannot directly solve the GDRASS with stop location, and a reliable algorithm requires to be developed to address this problem.

3. Methodology

3.1. Research framework

In this study, a GDRASS model is presented for the collaborative optimization of stop location, route design and departure time settings, so that all passengers are directed from their demand points to the selected stops and passengers at selected stops are conveniently delivered to the airport. Ridership and time windows of demand points and the real travel speed/distance matrix between demand points, shuttle stops, depots and the airport are the primary inputs of the model. Using a smart phone and a public geo-information system (GIS) facility, we are able to acquire the above primary input parameters. Each AS that departs from the depot and arrives at the airport, visits the selected stops to serve passengers in the boarding time windows. A penalty fee will be charged if an AS is ahead of schedule or delayed in arriving at the passenger's position. Factors that affect the carbon emissions of an AS include its speed, load weight as well as mileage [15]. Obviously, the speed of AS on the route

is affected by the degree of traffic congestion at different times, and its variation regularity can be represented by the sectional function. The primary goal of this research is to allocate all demand points to shuttle stops, route each AS departing from a depot, provide the selected stops and arrive at the airport, and figure out the times that each AS gets and departs all selected stops. The primary purpose of this study was to simultaneously minimize the total travel time of all passengers, the punishment expense of violating the time-window as well as carbon emissions.

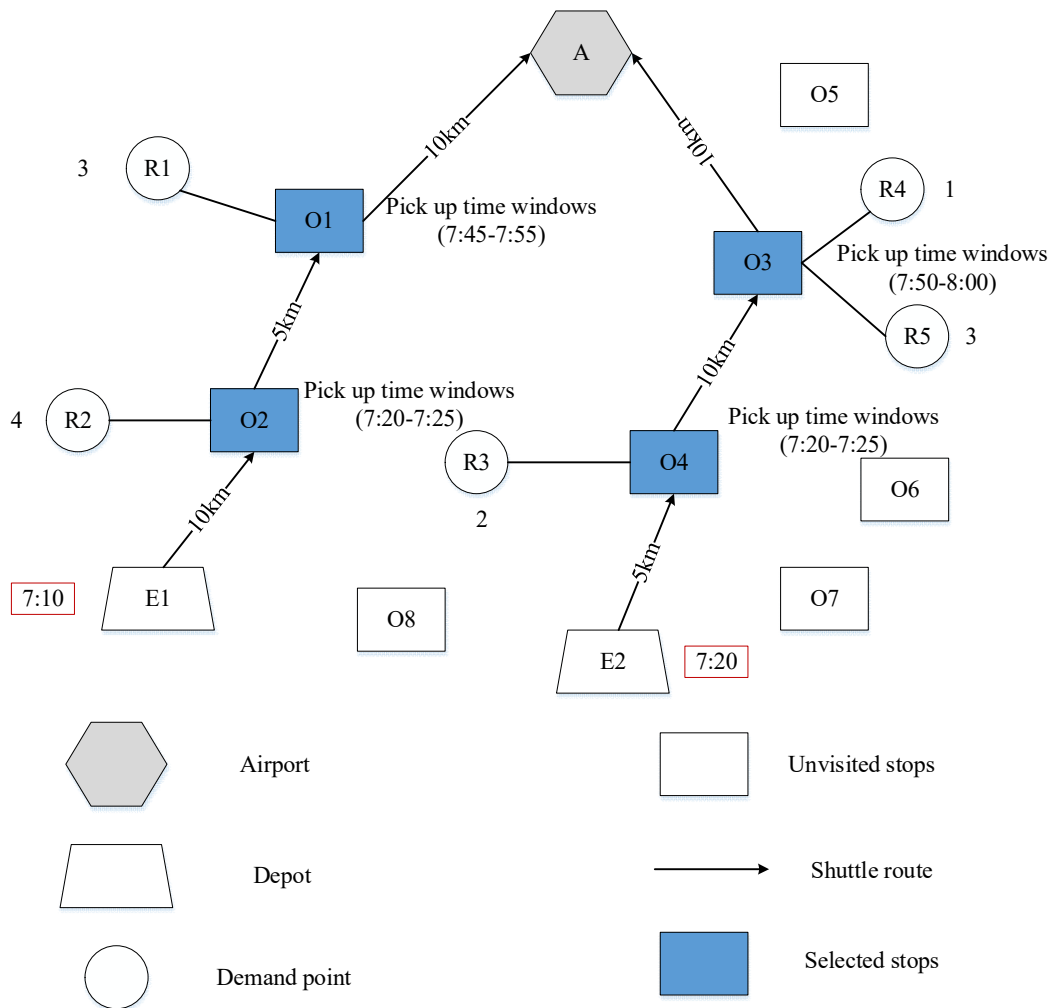


Figure 1. Visual expression of the GDRASS model.

Figure 1 provides a simple explanation of the GDRASS model. The GDRASS system contains one airport (A), five demand points (R1–R5), eight optional stops (O1–O8) and two depots (E1, E2). Figure 2 shows the time-dependent speed on different roads. Time windows are depicted by the numbers in brackets around each selected shuttle stop. The number of passengers at each demand point is depicted by the number surrounding the circle. The distance between two adjacent selected shuttle stops is indicated by the number embedded in the arrow. It takes one minute for all passengers to board the shuttle. The results of the optimization consist of three parts. The first part is the stop location, i.e., allocating demand points to the selected stops, represented by O1(R1), O2 (R2), O3 (R4, R5) and O4 (R3). Considering O3 (R4, R5) as an instance, the amount of passengers taking the shuttle at O3 was

the sum of those of R4 and R5. The second part is the departure time of shuttles from depots. The third part is the routing results. In this example, there are two shuttle routes, represented by (E1 (7:10)–O2 (7:30, 7:31)–O1 (7:46, 7:47)–A(8 :07)) and (E2 (7:20)–O4 (7:30, 7:31)–O3 (7:55,7:56)–A (8:16)). Take the first route as an example for the following explanation: Shuttle 1 leaves depot E1 at 7:10. Since the shuttle is traveling at 30 km/h on the road section E1-O2, the shuttle gets to O2 at 7:30 and leaves O2 at 7:31 at a speed of 20 km/h after loading 4 passengers. Apparently, the shuttle fails to arrive at the stop within the time window and is approximately 5 minutes delayed. Likewise, the shuttle gets to O1 at 7:46 and leaves at 7:47 after carrying three passengers. Lastly, it reaches airport A at 8:07 and unloads 7 passengers. In such a situation, the value of each objective function for all AS routes will be simply computed.

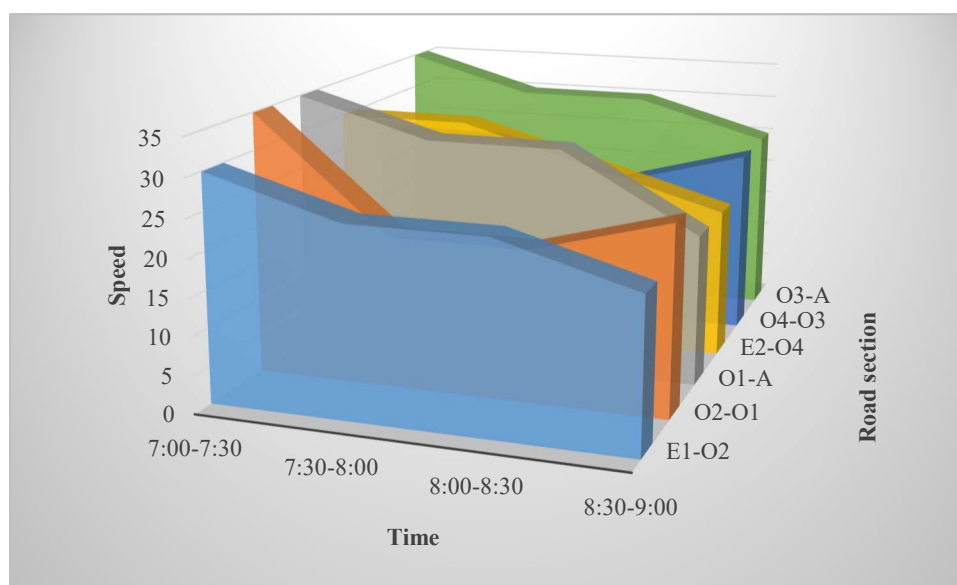


Figure 2. Time-dependent speed on different roads.

The next assumptions have been investigated in the presented GDRASS model in order to suit scenarios in reality well:

(i) Only one shuttle stop could be assigned to each demand point, and each stop can only be served once by an airport shuttle.

(ii) The unit expense of carbon emissions, and the unit time punishment expense of shuttles visiting the selected stop early or late can be evaluated.

(iii) The real interchange or travel distance/time matrix linking demand points, shuttle stops, depots and the airport along with time-dependent speed on the route can be acquired by using a public GIS facility.

3.2. Model formulation

3.2.1. Notation

To simplify the expression of the model, all definitions and notations utilized in the following are depicted in Table 1.

Table 1. Definitions and notations in the GDRASS model.

| Indices: | |
|---------------------|---|
| r | Demand point index |
| j, e | Shuttle node (depot, shuttle stop, and airport) index |
| s | Airport shuttle index |
| Sets: | |
| R | Set of demand points |
| S | Set of ASs |
| O | Set of optional stops |
| E | Set of depots |
| A | Set of airports |
| Parameters: | |
| p_r | Ridership at demand point r ; $\forall r \in R$ |
| Q | Upper bound of the AS capacity |
| D_{max} | Upper bound of the AS mileage |
| T_{min} | Minimum travel time of shuttle route |
| D_s | The total mileage of the AS s serving shuttle stops; $\forall s \in S$ |
| T_s | The total travel time of the AS s serving shuttle stops; $\forall s \in S$ |
| G | Maximum interchange distance |
| d_{rj} | Distance on the basis of the map from the airport, shuttle stops, and depots to demand points r and j ; $\forall r, j \in R \cup O \cup E \cup A$ |
| v | Average interchange speed |
| $v_{je}(t_j^s)$ | The piecewise function of travel speed from the shuttle node j to e , associated with the time of the AS s serving selected stop j ; $\forall s \in S \forall j, e \in A \cup E \cup O$ |
| ω_s | The weight of the AS s ; $\forall s \in S$ |
| θ | The mean weight of per passenger |
| T_j | Time of arriving shuttle stop j ; $\forall j \in O$ |
| $[a_j, l_j]$ | Time window of arriving the selected shuttle stop j ; $\forall j \in O$ |
| c_e | Punishment expense for early arrival |
| c_l | Punishment expense for late arrival |
| c_p | Unit carbon emission expense |
| f_p | Carbon emission coefficient |
| H | A large constant |
| Decision variables: | |
| z_j | Whether the optional stop j is selected as an AS stop; $\forall j \in O$ |
| h_{rj} | Whether the demand point r is allocated to an AS stop j ; $\forall r \in R, \forall j \in O$ |
| x_{je}^s | Whether the AS s visits the stop j before visiting the stop e ; $\forall s \in S, \forall j, e \in E \cup A \cup O$ |
| y_j^s | Whether the AS stop j is served by the AS s ; $\forall j \in O, \forall s \in S$ |
| t_j^s | The time of the AS s serving the AS stop j ; $\forall j \in E \cup A \cup O, \forall s \in S$ |
| p_j^s | Ridership at the AS stop j allocated to AS s ; $\forall j \in O, \forall s \in S$ |
| U_{js} | An auxiliary (real) variable for subroutes removal constraint in route of AS s ; $\forall j \in E \cup A \cup O, \forall s \in S$ |

3.2.2. Formulation

$$\min f_1 = \sum_{\forall r \in R} \sum_{\forall j \in O} h_{rj} \cdot \frac{d_{rj}}{v} \cdot p_r + \sum_{\forall j \in O} \sum_{\forall s \in S} y_j^s \cdot \sum_{\forall r \in R} h_{rj} \cdot p_r \cdot (T_s - t_j^s) \quad (1)$$

$$\min f_2 = c_p \cdot f_p \cdot \sum_{\forall j, e \in O \cup E \cup A} \sum_{\forall s \in S} x_{je}^s \cdot F(\omega_s + p_j^s, v_{je}(t_j^s), d_{je}) \quad (2)$$

$$\min f_3 = \sum_{\forall j \in O} \sum_{\forall s \in S} y_j^s \cdot p_j^s \cdot [c_e \cdot \max(a_j - t_j^s, 0) + c_l \cdot \max(t_j^s - l_j, 0)] \quad (3)$$

$$h_{rj} \leq z_j, \forall r \in R, \forall j \in O \quad (4)$$

$$\sum_{\forall j \in O} h_{rj} = 1, \forall r \in R \quad (5)$$

$$h_{rj} \cdot d_{rj} \leq G, \forall r \in R, \forall j \in O \quad (6)$$

$$y_j^s \leq z_j, \forall s \in S, \forall j \in O \quad (7)$$

$$\sum_{\forall j \in O} y_j^s \geq 1, \forall s \in S \quad (8)$$

$$\sum_{\forall j \in O} x_{je}^s = 1, \forall s \in S, \forall e \in A \quad (9)$$

$$\sum_{\forall j \in O} x_{ej}^s = 0, \forall s \in S, \forall e \in A \quad (10)$$

$$\sum_{\forall j \in O} x_{je}^s = 0, \forall s \in S, \forall e \in E \quad (11)$$

$$\sum_{\forall j \in O} x_{ej}^s = 1, \forall s \in S, \forall e \in E \quad (12)$$

$$\sum_{\forall e \in O \cup E \cup A} x_{je}^s = \sum_{\forall e \in O \cup E \cup A} x_{ej}^s = y_j^s, \forall s \in S, \forall j \in O \quad (13)$$

$$U_{js} - U_{es} |O \cup E \cup A| \cdot x_{je}^s \geq |O \cup E \cup A| - 1 \quad \forall s \in S, \forall j, e \in O \cup E \cup A \quad (14)$$

$$t_j^s + T_j + \frac{d_{je}}{v_{rj}(t_j^s)} + (1 - x_{je}^s)H \leq t_e^s, \forall s \in S, \forall j, e \in O \cup E \cup A \quad (15)$$

$$t_j^s + T_j + \frac{d_{je}}{v_{rj}(t_j^s)} - (1 - x_{je}^s)H \geq t_e^s, \forall s \in S, \forall j, e \in O \cup E \cup A \quad (16)$$

$$p_j^s + \sum_{\forall r \in R} h_{rj} \cdot p_r + (1 - x_{je}^s)H \leq p_e^s, \forall s \in S, \forall j, e \in O \cup E \cup A \quad (17)$$

$$p_j^s + \sum_{\forall r \in R} h_{rj} \cdot p_r - (1 - x_{je}^s)H \geq p_e^s, \forall s \in S, \forall j, e \in O \cup E \cup A \quad (18)$$

$$D_s = \sum_{\forall j,e \in O \cup E \cup A} x_{je}^s d_{je} \leq D_{max}, \forall s \in S \quad (19)$$

$$T_s = \sum_{\forall j,e \in O \cup E \cup A} x_{je}^s t_{je} \geq T_{min} \quad \forall s \in S \quad (20)$$

where $F(\omega_s + p_j^s, v_{je}(t_j^s), d_{je})$ is a carbon emissions function varying with speed of the airport shuttle from stop j to stop e when accounting for changes in traffic conditions. The speed $v_{je}(t_j^s)$ is a piecewise function.

$v_{je}(t_j^s)$ and its value is determined by t_j^s . $\omega_s + p_j^s$ represents the sum of shuttle weight and passengers weight departing from the stop j . Utilizing the equation presented by Demir et al. [15,19,28], this can be expressed as follows:

$$F(\omega_s + p_j^s, v_{je}(t_j^s), d_{je}) = 0.0308d_{je} \left\{ \frac{33}{v_{je}(t_j^s)} + 0.8175 + 0.2725(\omega_s + p_j^s \cdot \theta) + 0.0035v_{je}(t_j^s)^2 \right\} \quad (21)$$

Objective (1) is to ensure that the total travel time of passengers is minimized. Objective (2) is to minimize the expense of carbon emissions. Objective (3) is to minimize the punishment expense of violating the time-window. Equations (4) and (5) ensure that passengers at each demand point can only interchange to one selected stop. Equation (6) is the interchange distance constraint, i.e., the interchange distance does not surpass G . Equation (7) guarantees that each selected stop is served by shuttles. Equation (8) ensures that the minimum number of serviced stops along each shuttle route is 1. Equations (9)–(12) ensure that each shuttle starts at the depot and finally ends at the airport. Equation (13) represents that every selected stop can only be served by one shuttle. Equation (14) is utilized to eliminate the constraint of the sub-tour. Equations (15) and (16) determine the time when the airport shuttle b serves the present stop. Equations (17) and (18) compute the number of passengers carried by each shuttle when it arrives at each stop. Equations (19) and (20) indicate that the drive mileage and travel time for each shuttle must be within the specified range.

4. Solution method

The GDRASS is classified as a mixed-integer non-linear problem and it has been considered as NP-hard. Exact algorithms tend to have poor performance in terms of computational efficiency. Heuristics are frequently utilized by scholars to handle NP-hard problems [2,8,26]. Thus, a two-stage MOALO-based heuristic algorithm is presented in this section to solve the proposed model. Figure 3 exhibits the solution structure of the algorithm [29]. In the first stage, MOALO is utilized to allocate demand points to different airport shuttles and determine departure time of each AS. In the second stage, the greedy and dynamic programming algorithms are incorporated in MOALO to assign demand points to shuttle stops and decide the sequence of each AS visiting selected shuttle stops.

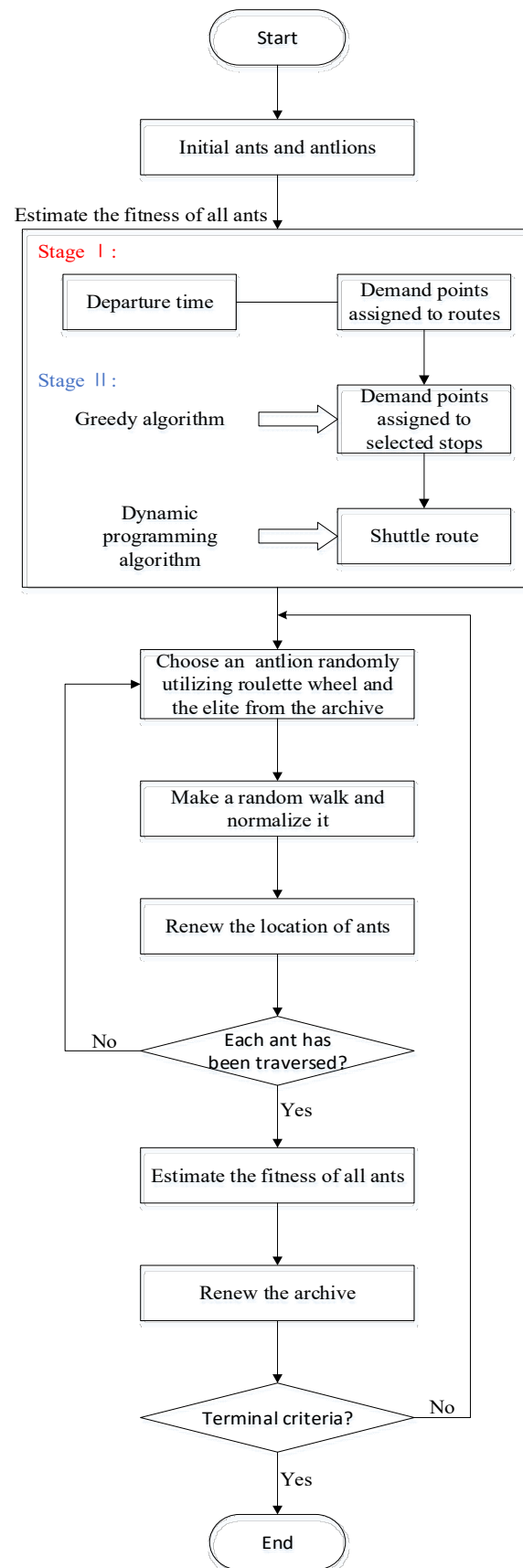


Figure 3. Flow diagram of the MOALO-based two-stage algorithm.

4.1. Coding scheme

We use the position of the ant $P = (p_1, p_2, \dots, p_{|R|}, p_{|R|+1}, \dots, p_{|R|+|S|})$, which consists of two sections, to denote the problem solution. The first section of the position of the ant X represents the scheme of different ASs service demand points. Therefore, each p_r ($1 \leq r \leq |R|$) represents that AS x_r serves demand point r . Each element of the second section of the position of the ant $p_{|R|+s}$ ($1 \leq s \leq |S|$) indicates the departure time of the AS b . As an example, a solution consisting of two airport shuttles and six demand points is represented as $P = \{2, 2, 1, 1, 2, 1; 6:30, 6:35\}$, in which the airport shuttle S_1 departs from the depot at 6:30 and serves demand points 3, 4 and 6; while S_2 departs from the depot at 6:35 and serves demand points 1, 2 and 5.

4.2. The solving process of the MOALO-based two-stage algorithm

In MOALO of the first stage, the origin location of the ant and antlion is generated randomly. In each iteration, an objective function is utilized to estimate the fitness of each ant and antlion. In the evaluation step, demand points are assigned to ASs, and the departure time of per shuttle is calculated. Following the preceding steps, the dynamic programming algorithm and greedy algorithm of the second stage are employed to allocate demand points to selected stops and decide the order of the selected stops for the shuttle service [26]. Thereafter, we are able to acquire the complete scheduling scenario and derive the fitness value of the objective function. During the iterative process, each ant will choose a random antlion using roulette wheel and the elite from the archive, which will be utilized collectively to renew the location of the ant. Then the radius of ants' random walk around the antlions will be renewed. In addition, each iteration requires minimum-maximum normality and a boundary checking. After above steps, the position of ants can be renewed by using the elitism mechanism. If each ant has finished these operations, evaluate the fitness of all ants. At last, renew the archive and examine the status. The optimal solution can be acquired after the end condition of the algorithm is satisfied [30].

In addition, the presented algorithm adopts punishment function to address optimization problems with constraints. The fitness value of an individual who violates the constraint will be replaced by a large constant [31].

$$F_1 = f_1 + H \cdot \sum_{r \in R, j \in E} \max\{h_{rj} \cdot d_{rj} - G, 0\} \quad (22)$$

$$F_2 = f_2 + H \cdot \sum_{s \in S} \left[\max\{\sum_{j, e \in O \cup E \cup A} x_{je}^s d_{je} - D_{max}, 0\} + \max\left\{T_{min} - \sum_{j, e \in O \cup E \cup A} x_{je}^s \cdot \frac{d_{je}}{v_{je}(t_j^s)}, 0\right\} \right] \quad (23)$$

$$F_3 = f_3 + H \cdot \sum_{s \in S} \max\{\sum_{j \in O} y_j^s p_j^s - Q, 0\} \quad (24)$$

5. Case study

5.1. Case description

In the case analysis, an illustrative case of designing GDRASS for Tianjin City in China is used to prove the feasibility of the proposed methodology. The GDRASS system in this case consists one

airport (A), five depots (E1–E5), 30 demand points (R1–R30) and 45 optional stops (O1–O45). Table 2 displays the quantity of passengers and their time windows at each demand point. The critical input data utilized in the case analysis are listed below:

- 1) Number of shuttles: 5.
- 2) Maximum capacity of each shuttle: $Q = 12$ per.
- 3) Maximum interchange distance: $G = 5$ km.
- 4) Weight of each shuttle: $\omega_s = 23,000$ kg.
- 5) Mean weight per passenger: $\theta = 60$ kg.
- 6) Punishment expense of early arrival: $c_e = 1$ CNY/min.
- 7) Punishment expense of late arrival: $c_l = 3$ CNY/min.
- 8) Unit carbon emission expense: $c_p = 80$ CNY/ton.
- 9) Carbon emission coefficient: $f_p = 0.785$ kg/liter.

Table 2. Ridership and time windows of demand points.

| No. | p_r | $[a_j, l_j]$ | No. | p_r | $[a_j, l_j]$ |
|-----|-------|--------------|-----|-------|--------------|
| R1 | 2 | [6:30–6:50] | R16 | 2 | [7:05–7:10] |
| R2 | 1 | [6:30–6:50] | R17 | 1 | [7:00–7:25] |
| R3 | 2 | [6:30–6:50] | R18 | 3 | [6:35–6:55] |
| R4 | 1 | [7:00–7:05] | R19 | 2 | [6:35–6:55] |
| R5 | 1 | [7:00–7:05] | R20 | 2 | [6:35–6:55] |
| R6 | 2 | [6:55–7:05] | R21 | 2 | [6:35–6:55] |
| R7 | 1 | [6:55–7:10] | R22 | 1 | [6:55–7:15] |
| R8 | 2 | [6:35–6:55] | R23 | 3 | [7:05–7:20] |
| R9 | 2 | [6:45–7:10] | R24 | 2 | [6:55–7:15] |
| R10 | 2 | [7:00–7:25] | R25 | 2 | [6:35–6:50] |
| R11 | 2 | [6:50–7:10] | R26 | 2 | [6:35–6:50] |
| R12 | 1 | [7:00–7:25] | R27 | 1 | [6:35–6:50] |
| R13 | 2 | [6:30–6:45] | R28 | 2 | [6:45–6:55] |
| R14 | 2 | [6:35–6:55] | R29 | 2 | [6:35–6:55] |
| R15 | 2 | [6:45–7:05] | R30 | 2 | [6:55–7:10] |

5.2. Results

Using the proposed model, we can acquire 10 Pareto optimal solutions in three dimensions, which contain route design, stop location and departure time setting. The maximum value of the total travel time is 1364 minutes and the minimum value is 1316.1 minutes, that of carbon emission expense are 1.6 and 1.3 CNY, and that of time window expense are 210 and 190.1 CNY, separately. The pairwise relationship between the three objectives is shown in Figure 4. Total travel time and carbon emission expense are positively relevant. The primary reasons are that the total in-vehicle time and the total expense of carbon emissions are both determined by route mileage and travel speed of AS. With the decrease of the total in-vehicle time, the total interchange time increases. However, the sum of the total in-vehicle time and the total interchange time decreases, thus the total travel time decreases. Time window expense decreases with the increase of carbon emission expense and total in-vehicle time. The primary reason is that the reduced total punishment expense of violating time windows of passengers

results in ASs requiring more mileages to respond to all selected stops, thereby increasing the total expense of carbon emission and total travel time.

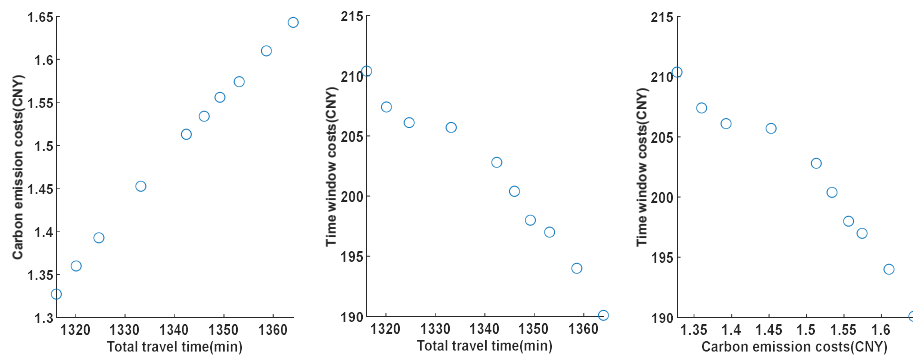


Figure 4. Pairwise relationship between the three objectives.

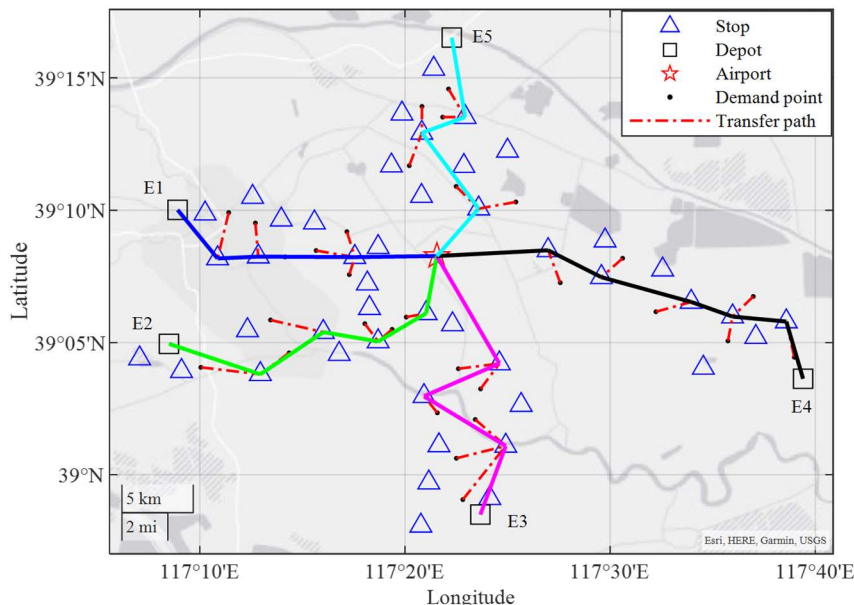


Figure 5. Graphical map of the optimal scheme.

Tables 3 and 4 illustrate the routing and scheduling results for the optimal scheme (1316.1, 1.3, 210). Table 3 provides the assigning results for all demand points to selected stops served by shuttles, including the interchange distance and early/delayed arrival time of the AS at each selected stop. Normal, late and early arrivals are indicated by zero, positive and negative figures in the fifth column of the table, respectively. Table 4 details the arriving and leaving time for five ASs serving their selected stops, total travel time of all passengers as well as carbon emissions of each AS. Considering the AS of S_1 as an instance, the AS departs the depot E1 at 6:27 and gets to the shuttle stop O2 at 6:35. Due to the passengers' time window is [6:30–6:50], the AS reaches the shuttle stop normally. It leaves selected stop O2 at 6:36 after picking up 2 passengers in one minute. Then, the AS arrives at the shuttle

stop O4 at 6:41 and leaves the shuttle stop at 6:42. The arrival and departure time of O7 is (6:59, 7:00). Due to the passengers at demand points R4, R5 and R6 need to interchange to the stop O4 to board the shuttle, thus the expense of violating time windows of O7 is the sum of that of R4, R5 and R6 (i.e., $1 \times 1 + 1 \times 1 + 0 = 2$ CNY). Finally, this AS reaches the airport A at 7:14 to drop off 9 passengers. As stated previously, the total travel time of passengers for O2, O4 and O7 are computed as 55.3 minutes, 90.2 minutes and 71.6 minutes. The mileage of the AS is 19.8 km, and the CO₂ emissions are 2.6 kg. The expense of carbon emissions is 0.2 CNY, and the punishment expense of time window violations is 2 CNY.

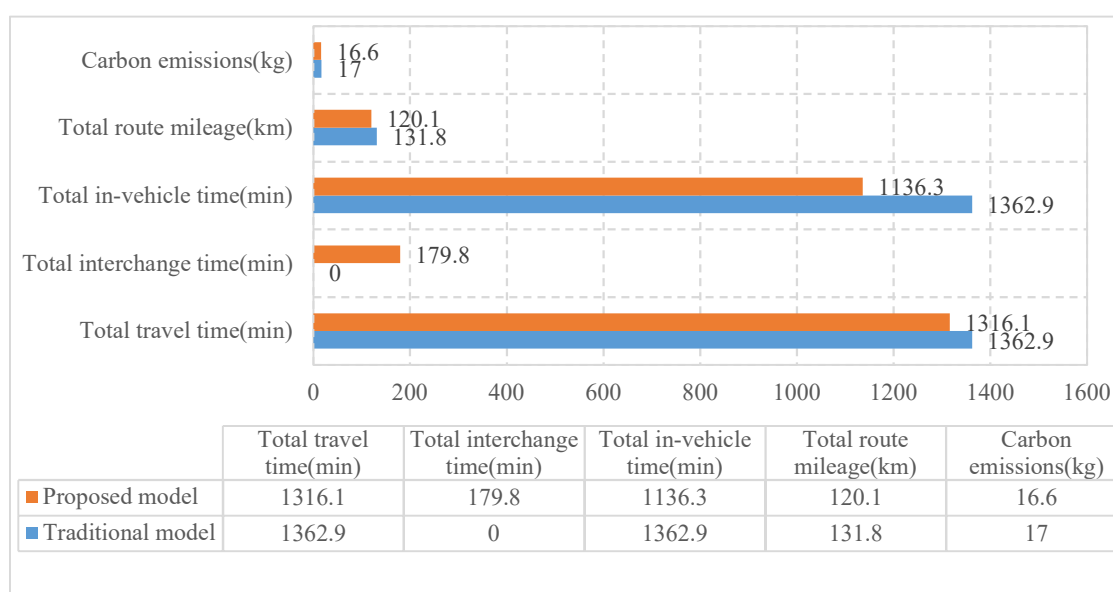
Table 3. Results of allocation for all demand points to selected stops served by shuttles.

| Demand point | Shuttle stop | Allocated AS | Interchange distance(km) | Early/late time(min) |
|--------------|--------------|--------------|--------------------------|----------------------|
| R1 | O2 | | 3.3 | 0 |
| R2 | O4 | | 2.4 | 0 |
| R3 | | | 1.9 | 0 |
| R4 | | S_1 | 2.8 | -1 |
| R5 | O7 | | 1.3 | -1 |
| R6 | | | 1.9 | 0 |
| R7 | O12 | | 3.8 | 0 |
| R8 | O14 | | 4.2 | 0 |
| R9 | | | 2.5 | 0 |
| R10 | | S_2 | 1.6 | 0 |
| R12 | O15 | | 1.3 | 0 |
| R11 | O17 | | 1.4 | 7 |
| R13 | | | 4.8 | 0 |
| R14 | O26 | | 3.6 | 0 |
| R18 | | | 2.8 | 0 |
| R15 | | S_3 | 2.2 | 3 |
| R16 | O25 | | 2.9 | -2 |
| R17 | | | 1.5 | -4 |
| R19 | O35 | | 2.0 | 0 |
| R21 | | | 1.7 | 0 |
| R20 | | | 2.6 | 0 |
| R22 | O33 | | 2.6 | 0 |
| R23 | | | 2.0 | 0 |
| R24 | | S_4 | 2.4 | 10 |
| R25 | O39 | | 2.3 | 0 |
| R27 | | | 1.6 | 0 |
| R26 | | | 1.9 | 2 |
| R28 | O40 | | 2.5 | 0 |
| R29 | | S_5 | 2.2 | 11 |
| R30 | O43 | | 2.6 | 0 |

Table 4. Routing and scheduling plans.

| AS | Sequence of stops served by shuttles | Total travel time (min) | Carbon emissions (kg) | Mileage (km) | Number of passengers |
|-------|---|-------------------------|-----------------------|--------------|----------------------|
| S_1 | E1(6:27)-O2(6:35-6:36)-O4(6:41-6:42)-O7(6:59-7:00)-A(7:14) | 231.9 | 2.6 | 19.8 | 9 |
| S_2 | E2(6:29)-O14(6:45-6:46)-O12(6:56-6:57)-O15(7:07-7:08)-O17(7:17-7:18)-A(7:28) | 265.9 | 3.3 | 24 | 10 |
| S_3 | E3(6:31)-O26(6:41-6:42)-O22(6:56-6:57)-O25(7:08-7:09)-A(7:26) | 340.6 | 3.9 | 26.4 | 12 |
| S_4 | E4(6:33)-O28(6:41-6:42)-O35(6:51-6:52)-O33(7:00-7:01)-O34(7:17-7:18)-O32(7:25-7:26)-A(7:39) | 318 | 3.9 | 30 | 12 |
| S_5 | E5(6:34)-O39(6:44-6:45)-O40(6:52-6:53)-O43(7:06-7:07)-A(7:18) | 159.7 | 2.9 | 19.9 | 11 |

Figure 5 provides a graphical map of shuttle routes and passenger guidance. The airport is indicated by a red star. All depots are indicated by black squares. All shuttle stops are indicated by blue triangles. All demand points are indicated by black dots. The deep blue solid line represents the shuttle route of S_1 , the green solid line represents the route of S_2 , the solid pink line represents the shuttle route of S_3 , the solid black line represents the shuttle route of S_4 , and the light blue solid line represents the route of S_5 . The red dotted lines between the selected blue triangles and black points are utilized to show the interchange paths of passengers.

**Figure 6.** Comparative results of the two models.

In addition, our proposed model is different from the traditional DRASS due to considering the stop location and time-dependent speed. Figure 6 illustrates the difference between the traditional model and our proposed model. In the proposed model, passengers need to interchange to the selected stop from the demand point, thus increasing the total interchange time. However, the amount of selected stops served by each shuttle reduced, leading to reduced total route mileage and the total in-vehicle time for passengers. Since the reduction in total in-vehicle time is greater than the growth in total interchange time, the total travel time of the proposed model is shorter than that of the conventional one. The presented model reduced carbon emissions by 2.4% in comparison to the conventional model. On the one hand, this is due to the reduction in the total route mileages of the proposed model. On the other hand, elastic departure time for each shuttle in a time-dependent road environment can prevent increased carbon emissions due to road congestion.

5.3. Sensitive analysis

Table 5 illustrates the performance comparison of the model for various amounts of airport shuttles. As the amount of airport shuttles increases, so do the unnecessary mileages and times, thus raising the total mileage of the route as the starting position of the route is the depot and the ending position is the airport. Nonetheless, with the increase in the amount of airport shuttles, each AS serves fewer stops, which reduces the total in-vehicle time for passengers. Equally, the reduction in the amount of stops served by such airport shuttles may result in shuttles getting to stops more quickly, thereby adding the total early and late arrival times. Owing to the appropriate demand points and stops distribution setting, the total interchange time stays the same for both models. The total travel time reduced as the sum of total in-vehicle time and the total interchange time became smaller. Carbon emissions increased due to the increasing total route mileages.

Table 5. Comparative results of various amount of airport shuttles.

| Scenario | Total travel time (min) | Total interchange time (min) | Total in-vehicle time (min) | Carbon emissions (kg) | Time window expense (CNY) | Mileage (km) |
|------------|-------------------------|------------------------------|-----------------------------|-----------------------|---------------------------|--------------|
| 5 shuttles | 1316.1 | 179.8 | 1136.3 | 16.6 | 210 | 120.1 |
| 6 shuttles | 1297 | 179.8 | 1117.2 | 17.1 | 221 | 134.8 |
| 7 shuttles | 1283.5 | 179.8 | 1103.7 | 17.5 | 229 | 147.2 |

Table 6. Comparative results of various weight factor c_l/c_e .

| Scenario | Mileage (km) | Carbon emissions (kg) | Early arrival time (min) | Late arrival time (min) |
|----------|--------------|-----------------------|--------------------------|-------------------------|
| 1:1 | 121.4 | 17.0 | 8 | 79 |
| 2:1 | 120.1 | 16.6 | 11 | 73 |
| 3:1 | 120.1 | 16.6 | 12 | 71 |
| 4:1 | 117.2 | 16.3 | 18 | 56 |

Table 6 analyzes how the weight factor c_l/c_e affect the results of the model. With the gradual increase in weight coefficient, there will be more early arrivals and fewer delayed arrivals. In addition, total mileage and carbon emissions stay unchanged before reaching the boundary value. Once the

boundary value is reached, the GDRASS scheme would result in less carbon emissions due to the reduction of mileage. The primary reason is that the increase in the weight factor c_l/c_e leads to more early arrival time and less delayed arrival time, resulting in a decrease in the route mileage.

5.4. Algorithm validations

To validate the effectiveness of the proposed algorithm, the solutions of the proposed algorithm are compared with other four algorithms: multi-objective artificial bee colony (MOABC) [32], multi-objective multiverse optimization algorithm (MOMVO) [33], multi-objective particle swarm optimization (MOPSO) [34] and nondominated sorting genetic algorithm II (NSGA-II) [26]. Hypervolume (HV) is a well-used indicator for evaluating the performance of algorithms [35]. The higher the HV value of each algorithm is, the better its convergence and diversity. In this study, HV values and computation time are utilized to compare the solution quality and computation speed of each algorithm at different problem scales. Table 7 illustrates the comparison results, from which we can see: As more demand points are served, the HV value of each algorithm tends to decrease, and the computation time of each algorithm is longer. However, the HV value of the proposed algorithm is the highest compared with the other four algorithms at different problem scales. The computation time of the proposed algorithm is shorter than that of the other four algorithms at all problem scales. In conclusion, the proposed algorithm performs better in terms of computing speed and quality of solutions.

Table 7. Comparison in computation quality and efficiency of different algorithms.

| Scale of the problem | Algorithms | HV | Computation time (s) | Increased time (%) |
|----------------------|--------------------|------|----------------------|--------------------|
| 30 | Proposed algorithm | 10.1 | 132.2 | — |
| | MOABC | 9.7 | 134.4 | 1.7 |
| | MOMVO | 9.1 | 138.9 | 5.1 |
| | MOPSO | 9.6 | 136.8 | 3.5 |
| | NSGA-II | 9.5 | 137.3 | 3.9 |
| 60 | Proposed algorithm | 10.0 | 149.3 | — |
| | MOABC | 9.4 | 155.3 | 4.0 |
| | MOMVO | 9.0 | 158.4 | 6.1 |
| | MOPSO | 9.5 | 153.9 | 3.1 |
| | NSGA-II | 9.4 | 156.9 | 5.1 |
| 120 | Proposed algorithm | 9.9 | 162.8 | — |
| | MOABC | 9.3 | 170.3 | 4.6 |
| | MOMVO | 8.9 | 173.3 | 6.4 |
| | MOPSO | 9.4 | 169.9 | 4.4 |
| | NSGA-II | 9.3 | 171.6 | 5.4 |

6. Conclusions

We proposed a multi-objective optimization model for green demand responsive airport shuttle

scheduling with stop location to balance the service level, economic expense and environmental expense. The proposed model could simultaneously assign demand points to selected stops and routing shuttles to visit these stops in time windows to transport all passengers from their home or work places to the airport. Depending on the features of the optimal model, we provided a two-stage MOALO-based algorithm combining the dynamic programming algorithm and greedy algorithm to obtain the Pareto-optimal solutions. The MOALO algorithm was utilized to assign demand points to ASs and decide when the AS leave the depot in stage I. By inserting dynamic programming algorithm and greedy algorithm in MOALO, demand points are assigned to selected stops and the order of selected stops serviced by each AS is calculated in stage II. The practicability and applicability of the presented model and algorithm were demonstrated by an actual case. Results revealed that the proposed model had a notable decrease of 3.4% in total passenger travel time and 2.4% in carbon emissions in comparison to the traditional one. The findings demonstrated that the presented model could optimize stop selection and green demand responsive airport shuttle scheduling. Further, sensitivity analysis was conducted to explore how the number of shuttle routes and the weight factor c_l/c_e impacted the performance of the model.

It is noticeable that the shuttle in the GDRASS model is a gasoline vehicle, rather than an electric vehicle (EV). The EV has virtually zero carbon emissions, but it can be charged at any usable stop in non-operating times. Under such a circumstance, integrated GDRASS route planning and charging stop location requires accounting for the relationship of the building and maintenance costs of charging stops and the operating fees of EVs. Therefore, the integration of charging stop location and EV route design in the GDRASS model is a worthwhile direction for further studying.

Use of AI tools declaration

The authors declare they have not used Artificial Intelligence (AI) tools in the creation of this article.

Acknowledgments

We acknowledge all of the people who have contributed to this paper in some manner. This study was jointly supported by the Tianjin Education Commission Natural Science Foundation (2021ZD004).

Conflict of interest

The authors declare there is no conflict of interest.

References

1. R. Q. Zhao, W. Liu, F. N. Zhang, T. T. R. Koo, G. Lodewijks, Passenger shuttle service network design in an airport, *Transportmetrica B: Transport Dyn.*, **10** (2022), 1099–1125. <https://doi.org/10.1080/21680566.2021.2008279>
2. X. Li, T. Wang, W. Xu, H. Li, Y. Yuan, A novel model and algorithm for designing an eco-oriented demand responsive transit (DRT) system, *Transp. Res. Part E Logist. Transp. Rev.*, **157** (2022), 102556. <https://doi.org/10.1016/j.tre.2021.102556>

3. Y. Yu, S. Wang, J. Wang, M. Huang, A branch-and-price algorithm for the heterogeneous fleet green vehicle routing problem with time windows, *Transp. Res. Part B Methodol.*, **122** (2019), 511–527. <https://doi.org/10.1016/j.trb.2019.03.009>
4. X. Li, M. Wei, J. Hu, Y. Yuan, H. Jiang, An agent-based model for dispatching real-time demand-responsive feeder bus, *Math. Probl. Eng.*, **2018** (2018). <https://doi.org/10.1155/2018/6925764>
5. B. Sun, M. Wei, W. Wu, An optimization model for demand-responsive feeder transit services based on ride-sharing car, *Information*, **10** (2019), 370. <https://doi.org/10.3390/info10120370>
6. Y. Xiao, A. Konak, The heterogeneous green vehicle routing and scheduling problem with time-varying traffic congestion, *Transp. Res. Part E Logist. Transp. Rev.*, **88** (2016), 146–166. <https://doi.org/10.1016/j.tre.2016.01.011>
7. A. K. Beheshti, S. R. Hejazi, A novel hybrid column generation-metaheuristic approach for the vehicle routing problem with general soft time window, *Inf. Sci.*, **316** (2015), 598–615. <https://doi.org/10.1016/j.ins.2014.11.037>
8. M. Wei, B. Jing, J. Yin, Y. Zang, A green demand-responsive airport shuttle service problem with time-varying speeds, *J. Adv. Transp.*, **2020** (2020). <https://doi.org/10.1155/2020/9853164>
9. Y. K. Xia, Z. Fu, Improved tabu search algorithm for the open vehicle routing problem with soft time windows and satisfaction rate, *Cluster Comput.*, **22** (2019), S8725–S8733. <https://doi.org/10.1007/s10586-018-1957-x>
10. J. P. Xu, F. Yan, S. Li, Vehicle routing optimization with soft time windows in a fuzzy random environment, *Transp. Res. Part E Logist. Transp. Rev.*, **47** (2011), 1075–1091. <https://doi.org/10.1016/j.tre.2011.04.002>
11. J. Zhang, Y. Zhao, W. Xue, J. Li, Vehicle routing problem with fuel consumption and carbon emission, *Int. J. Prod. Econ.*, **170** (2015), 234–242. <https://doi.org/10.1016/j.ijpe.2015.09.031>
12. J. Li, D. P. Wang, J. H. Zhang, Heterogeneous fixed fleet vehicle routing problem based on fuel and carbon emissions, *J. Cleaner Prod.*, **201** (2018), 896–908. <https://doi.org/10.1016/j.jclepro.2018.08.075>
13. M. Wen, W. Sun, Y. Yu, J. Tang, K. Ikou, An adaptive large neighborhood search for the larger-scale multi depot green vehicle routing problem with time windows, *J. Cleaner Prod.*, **374** (2022), 133916. <https://doi.org/10.1016/j.jclepro.2022.133916>
14. D. Zhang, X. Wang, S. Li, N. Ni, Z. Zhang, Joint optimization of green vehicle scheduling and routing problem with time-varying speeds, *PLoS One*, **13** (2018), e0192000. <https://doi.org/10.1371/journal.pone.0192000>
15. E. Demir, T. Bektas, G. Laporte, A review of recent research on green road freight transportation, *Eur. J. Oper. Res.*, **237** (2014), 775–793. <https://doi.org/10.1016/j.ejor.2013.12.033>
16. M. Adelzadeh, V. M. Asl, M. Koosha, A mathematical model and a solving procedure for multi-depot vehicle routing problem with fuzzy time window and heterogeneous vehicle, *Int. J. Adv. Manuf. Technol.*, **75** (2014), 793–802. <https://doi.org/10.1007/s00170-014-6141-8>
17. J. Brito, F. J. Martínez, J. A. Moreno, J. L. Verdegay, An ACO hybrid metaheuristic for close-open vehicle routing problems with time windows and fuzzy constraints, *Appl. Soft Comput.*, **32** (2015), 154–163. <https://doi.org/10.1016/j.asoc.2015.03.026>
18. N. Norouzi, M. Sadegh-Amalnick, R. Tavakkoli-Moghaddam, Modified particle swarm optimization in a time-dependent vehicle routing problem: minimizing fuel consumption, *Optim. Lett.*, **11** (2017), 121–134. <https://doi.org/10.1007/s11590-015-0996-y>

19. D. Wu, J. Li, J. Cui, D. Hu, Research on the time-dependent vehicle routing problem for fresh agricultural products based on customer value, *Agriculture*, **13** (2023), 681. <https://doi.org/10.3390/agriculture13030681>
20. H. Luo, M. Dridi, O. Grunder, A branch-price-and-cut algorithm for a time-dependent green vehicle routing problem with the consideration of traffic congestion, *Comput. Ind. Eng.*, **177** (2023), 109093. <https://doi.org/10.1016/j.cie.2023.109093>
21. F. Zhao, B. Si, Z. Wei, T. Lu, Time-dependent vehicle routing problem of perishable product delivery considering the differences among paths on the congested road, *Oper. Res.*, **23** (2023). <https://doi.org/10.1007/s12351-023-00751-3>
22. B. Ma, D. Hu, Y. Wang, Q. Sun, L. He, X. Chen, Time-dependent vehicle routing problem with departure time and speed optimization for shared autonomous electric vehicle service, *Appl. Math. Modell.*, **113** (2023), 333–357. <https://doi.org/10.1016/j.apm.2022.09.020>
23. S. Zhang, Z. Zhou, R. Luo, R. Zhao, Y. Xiao, Y. Xu, A low-carbon, fixed-tour scheduling problem with time windows in a time-dependent traffic environment, *Int. J. Prod. Res.*, **61** (2023), 6177–6196. <https://doi.org/10.1080/00207543.2022.2153940>
24. C. Ye, F. Liu, Y. K. Ou, Z. Xu, Optimization of vehicle paths considering carbon emissions in a time-varying road network, *J. Adv. Transp.*, **2022** (2022). <https://doi.org/10.1155/2022/9656262>
25. O. Jabali, T. Van Woensel, A. G. D. Kok, Analysis of travel times and CO2 emissions in time-dependent vehicle routing, *Prod. Oper. Manage.*, **21** (2012), 1060–1074. <https://doi.org/10.1111/j.1937-5956.2012.01338.x>
26. M. Wei, C. Yang, T. Liu, An integrated multi-objective optimization for dynamic airport shuttle bus location, route design and departure frequency setting problem, *Int. J. Environ. Res. Public Health*, **19** (2022), 14469. <https://doi.org/10.3390/ijerph192114469>
27. M. Wei, T. Liu, B. Sun, B. Jing, Optimal integrated model for feeder transit route design and frequency-setting problem with stop selection, *J. Adv. Transp.*, **2020** (2020). <https://doi.org/10.1155/2020/6517248>
28. X. Luo, L. Dong, Y. Dou, Y. Li, K. Liu, J. Ren, et al., Factor decomposition analysis and causal mechanism investigation on urban transport CO2 emissions: Comparative study on Shanghai and Tokyo, *Energy Policy*, **107** (2017), 658–668. <https://doi.org/10.1016/j.enpol.2017.02.049>
29. C. Dhifaoui, O. Kahouli, H. H. Abdallah, Multi-objective ant lion optimizer to solve the dynamic economic dispatch problem with valve point effect, in *19th International Conference on Sciences and Techniques of Automatic Control and Computer Engineering*, (2019), 564–571. <https://doi.org/10.1109/STA.2019.8717301>
30. S. Mirjalili, P. Jangir, S. Saremi, Multi-objective ant lion optimizer: a multi-objective optimization algorithm for solving engineering problems, *Appl. Intell.*, **46** (2017), 79–95. <https://doi.org/10.1007/s10489-016-0825-8>
31. X. B. Li, L. C. Yang, L. C. Huang, C. Wang, Dynamic multiobjective optimization and multivariate analysis for power generation scheduling of the diesel generators in dynamically positioned vessels, *Appl. Ocean Res.*, **122** (2022), 103132. <https://doi.org/10.1016/j.apor.2022.103132>
32. R. Akbari, R. Hedayatzadeh, K. Ziarati, B. Hassanizadeh, A multi-objective artificial bee colony algorithm, *Swarm Evol. Comput.*, **2** (2012), 39–52. <https://doi.org/10.1016/j.swevo.2011.08.001>

33. K. Kasturi, C. K. Nayak, M. R. Nayak, Electric vehicles management enabling G2V and V2G in smart distribution system for maximizing profits using MOMVO, *Int. Trans. Electr. Energy Syst.*, **29** (2019), e12013. <https://doi.org/10.1002/2050-7038.12013>
34. R. J. Kuo, M. F. Luthfiansyah, N. A. Masrurroh, F. E. Zulvia, Application of improved multi-objective particle swarm optimization algorithm to solve disruption for the two-stage vehicle routing problem with time windows, *Expert Syst. Appl.*, **225** (2023), 120009. <https://doi.org/10.1016/j.eswa.2023.120009>
35. A. P. Guerreiro, C. M. Fonseca, L. Paquete, The hypervolume indicator: Computational problems and algorithms, *ACM Comput. Surv.*, **54** (2021). 119. <https://doi.org/10.1145/3453474>



AIMS Press

©2023 the Author(s), licensee AIMS Press. This is an open access article distributed under the terms of the Creative Commons Attribution License (<http://creativecommons.org/licenses/by/4.0>)